Supplementary Information

Animal study

WT, *Shp*$^{-/-}$, and *Bhmt*$^{-/-}$ mice were reported previously [1, 2]. *Bhmt*$^{-/-}$*Shp*$^{-/-}$ double knockouts were generated by intercrossing heterozygous *Bhmt*$^{+/-}$ with *Shp*$^{+/-}$ mice and siblings were used for subsequent experiments. All mice used in this study had the genetic background of C57BL/6. The mice were maintained in a 12h/12h light/dark (LD) cycle (light on 6 AM to 6 PM) with free access to food and water. Experiments were performed on male mice at the age of 8 to 12 weeks. Serum and liver tissues were harvested at Zeitgeber time ZT2, ZT6, ZT10, ZT14, ZT18, and ZT22. A dim red light at intensity of 1 μmol/m^{2}s was used to collect tissues in dark condition. For alcohol-induced hyperhomocysteinemia, the NIAAA binge model [3] was used with sligh modification. In brief, after acclimatization of control liquid diet for 5 days, the mice were given control liquid diet (Bio-Serv, product #F1259SP) or 5% Lieber-DeCarli ethanol liquid diet (Bio-Serv, product #F1258SP) for 10 days, followed by oral gavage of a single dose of maltose (CTRL, 9g maltose dextrin/kg of body weight) or ethanol (EtOH, 5g ethanol/kg of body weight) solutions at 9 am on day 10. Nine hours after the binge, liver tissues and blood samples were collected every 6h over a 24h LD cycle at ZT12, ZT18, ZT0 and ZT6. For the induction of hyperhomocysteinemia with Hcy water, the mice were fed a normal pellet diet, but supplied with drinking water containing 0.18% of DL-Hcy (TCI America, Portland, OR, USA) for four weeks [4]. Glucose tolerance test was performed at 10 am by oral administration of glucose solution (2 mg/g body wt) to mice fasted for 16h. Blood glucose levels were measured by a blood glucose meter (Germaine Laboratories, San Antonio, TX, USA). Protocols for the animal experiments were approved by the Institutional Animal Care and Use Committee at the University of Utah.

Cell culture

Mouse hepatoma cell line Hepa1-6 (CRL-1830; American Type Culture Collection (ATCC), Manassas, VA, USA), and human cervix adenocarcinoma cell line HeLa (CCL-2; ATCC) were maintained in Dulbecco's modified Eagle's medium (DMEM) (Invitrogen, Carlsbad, CA, USA) with 10% heat-inactivated fetal bovine serum (Invitrogen). All transfection experiments were performed with X-tremeGENE HP reagent (Roche, Indianapolis, IN, USA). Hepa1-6 cells stably expressing FoxA1 was established by transfection with a FoxA1-expressing plasmid (described below), and selected and maintained in DMEM containing 600 μg/mL of G418 (Invitrogen), along with mock-transfected control cells (p3×FLAG-CMV-10; Sigma-Aldrich, St Louis, MO, USA).

Plasmid construction

All primers used for the plasmid construction and site-directed mutagenesis were summarized in Supplementary Table 1. Mouse Bhmt and Cth promoters were amplified by Takara LA Taq Polymerase (TaKaRa Bio USA, Madison, WI, USA) using C57BL/6 genomic DNA as a template. Following ristriction enzyme digestion, the PCR products were ligated into pGL3-basic (Promega, Madison, WI, USA), and sequence was confirmed. Site-directed mutagenesis of the mouse Bhmt promoter in pGL3 vector was performed by QuikChange Site-Directed Mutagenesis Kit (Stratagene, La Jolla, CA, USA). Mouse FoxA1 and FoxA2 coding regions were amplified from pGCDNsam-Foxa1-IRES-GFP and pGCDNsam-Foxa2-IRES-GFP (Addgene, Cambridge, MA, USA) [5], respectively, and were subcloned into p3×FLAG-CMV-10. The mouse Shp-expressing plasmid and adenovirus vector were described previously [6].

RNA isolation, next-generation RNA sequencing, and quantitative PCR

Total and 5' capped RNA purification from mouse liver and the PCR libraries used for RNA sequencing were as previously described [7]. Single 36 bp reads were obtained using the Illumina RNA sequencing protocol. Following cDNA synthesis with High-Capacity cDNA Reverse

Transcription Kit (Applied Biosystems, Foster City, CA, USA), quantitative PCR was carried out using the SYBR Green PCR master mix (Applied Biosystems) with primers shown in Supplementary Table 1. The amount of PCR products was measured by threshold cycle (Ct) values, and the relative ratio of specific genes to Hprt1 for each sample was then calculated.

Western blot

The following antibodies were used: β-actin (Sigma-Aldrich, A1978), Bhmt (Abcam, Cambridge, MA, USA, ab52144), Cth (Abcam, Danvers, MA, USA, ab80643), FoxA1 (Abcam, ab40868), Grp78 (Cell Signaling Technology, #3177), Ire1α (Cell Signaling Technology, #3294), phospho-Ire1 (Abcam, ab104157), Perk (Cell Signaling Technology, #3192), phospho-Perk (Cell Signaling Technology, #3179), Shp (Santa Cruz, sc-30169), β-tubulin (Cell Signaling Technology, #2128). Cells and liver tissues were lysed in RIPA buffer (50 mM Tri-HCl (pH 8.0), 150 mM NaCl, 1% Nonidet P-40, 0.1% sodium dodecylsulfate (SDS), 0.5% sodium deoxycholate) with protease inhibitors (PIs, Sigma-Aldrich). The lysates were separated by SDS-polyacrylamide gel electrophoresis and transferred to nitrocellulose membranes (Bio-Rad, Hercules, CA, USA). The membranes were blocked with TBS-T (20 mM Tris, 150 mM NaCl, 0.1% tween-20) containing 5% of blocking reagent (Bio-Rad), and incubated with primary antibodies followed by the incubation with horseradish peroxidase-conjugated corresponding secondary antibody. Antibody binding was visualized with SuperSignal West Pico Chemiluminescent Substrate (Fisher Scientific) according to the manufacturer's protocol. Equal loading of protein was verified with β-actin or β-tubulin.

ChIP assay

Liver tissues were fixed in 1% formaldehyde in phosphate-buffered saline for 15 min, and glycine solution was added at the final concentration of 125 mM. The fixed tissues were lysed with cell lysis buffer (50 mM Hepes-KOH (pH 8.0), 1 mM ethylenediaminetetraacetate (EDTA), 0.5 mM ethyleneglycoltetraacetate, 140 mM NaCl, 10% glycerol, 0.5% Nonidet P-40, 0.25% triton X-100, plus PIs) to isolate nuclei. The nuclei were washed with nuclei wash buffer (10 mM Tris-HCl (pH 8.0), 1 mM EDTA, 0.5 mM EGTA, 200 mM NaCl, plus PIs) followed by lysis in nuclei lysis buffer (50 mM Tris-HCl (pH 8.0), 10 mM EDTA, 1% SDS, plus PIs). Chromatin fragments were prepared by MicrosonTM XL-2000 Ultrasonic Cell Disruptor (Misonic Inc., Farmingdale, NY, USA). Following preclear with Dynabeads-protein G (Invitrogen), sheared chromatin was mixed with anti-FoxA1 antibody (Abcam, ab5089), and incubated at 4ºC overnight, along with no-antibody control. The chromatin-antibody complexes were precipitated with Dynabeads-protein G. The precipitates were washed once with RIPA-150 (50 mM Tri-HCl (pH 8.0), 150 mM NaCl, 1 mM EDTA, 0.1% SDS, 1% triton X-100, 0.1% sodium deoxycholate), twice with RIPA-500 (50 mM Tri-HCl (pH 8.0), 500 mM NaCl, 1 mM EDTA, 0.1% SDS, 1% triton X-100, 0.1% sodium deoxycholate), twice with RIPA-LiCl (50 mM Tri-HCl (pH 8.0), 500 mM LiCl, 1 mM EDTA, 1% Nonidet P-40, 1% triton X-100, 0.7% sodium deoxycholate), and twice with TE buffer (10 mM Tris-HCl (pH 8.0), 1 mM EDTA). The beads were resuspended in direct elution buffer (10 mM Tri-HCl (pH 8.0), 300 mM NaCl, 5 mM EDTA, 0.5% SDS), and incubated with RNase A (Sigma-Aldrich) at 65ºC for overnight followed by digestion with proteinase K (Invitrogen; 55ºC, 2hr). Chromatin DNA fragments were purified with QIAGEN PCR purification kit (Qiagen, Valencia, CA, USA), and subjected to qPCR using primers listed in Supplementary Table 1. The relative FoxA1 binding (ChIP enrichment) was calculated as: 2^[-Ct(FoxA1) + Ct(input)] - 2^[-Ct(no antibody) - Ct(input)] × 100. It was confirmed that non-specific binding was negligible, as the values obtained by primers about 3 kb away from the FoxA1 binding sites in the Bhmt or Cth promoters were 100-fold less than those of primers for the FoxA1 binding sites (data not shown).

Metabolomics analysis

To prepare serum samples for GC/MS, 360 µL of -20℃ 90% methanol (aq.) was added to 40 µL of serum to give a final concentration of 80% methanol. The samples were incubated for one hour at -20℃ followed by centrifugation at 30,000 x g for 10 minutes using a rotor chilled to -20℃. The supernatant containing the extracted meta bolites was then transferred to fresh disposable tubes and completely dried *en vacuo*. All GC-MS analysis was performed with a Waters GCT Premier mass spectrometer fitted with an Agilent 6890 gas chromatograph and a Gerstel MPS2 autosampler. Dried samples were suspended in 40 µL of a 40 mg/mL O-methoxylamine hydrochloride (MOX) in pyridine and incubated for one hour at 30℃. 25 µL of this solution was added to autosampler vials. 40 µL of N-methyl-N-trimethylsilyltrifluoracetamide (MSTFA) was added automatically via the autosampler and incubated for 60 minutes at 37℃ with shaking. After incubation 3 µL of a fatty acid methyl ester standard solution was added via the autosampler then 1 µL of the prepared sample was injected to the gas chromatograph inlet in the split mode with the inlet temperature held at 250℃. A 10:1 split ratio was used for analysis. The gas chromatograph had an initial temperature of 95℃ for one minute followed by a 40℃/min ramp to 110℃ and a hold time of 2 minut es. This was followed by a second 5℃/min ramp to 250℃, a third ramp to 350℃, then a final hold time of 3 minutes. A 30 m Phenomex ZB5-5 MSi column with a 5 m long guard column was employed for chromatographic separation. Helium was used as the carrier gas at 1 mL/min. Due to the dynamic concentration range of metabolites each sample was analyzed a second time at a more dilute 100:1 split ratio. Data was collected using MassLynx 4.1 software (Waters). The targeted approach for known metabolites was used for first pass data analysis. Metabolites were identified and their peak area was recorded using QuanLynx. Metabolite identity was established using a combination of an in house metabolite library developed using pure purchased standards and the commercially available NIST library. The data was normalized by mean centering to the internal standard d4-succinate.

Determination of liver enzymatic activities

For Bhmt enzymatic activity, liver pulverized in liquid nitrogen were homogenized in Tris buffer using a motorized tissue homogenizer (Talboys Engineering Corporation, Montrose, PA). Bhmt activity was measured as the conversion of [^{14}C]betaine to [^{14}C]methionine and [^{14}C]dimethylglycine as previously described [1]. The Cth activity was assessed as previously described [8]. Measurement of H2S Concentration in Plasma was performed as previously reported [9].

Quantification of liver metabolites

Plasma was spiked with stable labeled internal standards of all the analytes, and extracted using the method modified from Bligh and Dyer. Samples were extracted with methanol/chloroform (2:1, v/v), vortexed and incubated at -20℃ overnight. Samples were centrifuged and the supernatants re-extracted with methanol/chloroform/water (2:1:0.8, v/v/v). After vortexing and centrifugation, supernatants were combined with the first extract. Water and chloroform were added into the resulting solutions to allow the phase separation. After centrifugation, the aqueous phase containing choline, phosphocholine, glycerophosphocholine, betaine, TMAO, creatinine and methionine is ready for analysis. The organic phase (containing phosphatidylcholine and sphingomyelin) was diluted 1:10 diluted with methanol prior to analysis. Quantification of the analytes was performed using liquid chromatography-stable isotope dilution-multiple reaction monitoring mass spectrometry (LC-SID-MRM/MS). Chromatographic separations were performed on an Atlantis Silica HILIC 3 µm 4.6×50 mm column (Waters Corp, Milford, USA) using a Waters ACQUITY UPLC system. Column temperature was 40℃, and the flow rate 1 mL/min. The mobile phases were: A: 10% acetonitrile/90% water with 10 mM ammonium formate, 0.125% formic acid, and B: 90% acetonitrile/10% water, 10 mM ammonium formate, 0.125% formic acid. For aqueous analytes, the gradient was a5% A for 0.05 min, to

15% A in 0.35 min, to 20% A in 0.6 min, to 30% A in 1 min, to 45% A in 0.55 min, to 55% A in 0.05 min, at 55% A for 0.9 min, to 5% A in 0.05 min, at 5% A for 1.45 min. For the organic analytes, the gradient was 5% A for 0.05min, to 20% A in 2.95 min, to 55% A in 0.05 min, at 55% A for 0.95 min, to 5% A in 0.05 min, and at 5% A for 2.95 min. The analytes and their corresponding isotopes were monitored on a Waters TQ detector using characteristic precursor-product ion transitions. Concentrations of each analyte in samples were determined using the peak area ratio of the analyte to its isotope. Cystathionine and cysteine measurements were done by Dr. Sally Stabler at the University of Colorado. Briefly, these compounds were extracted from pulverized liver, isolated with the use of an anion-exchange column, derivatized with *N*-methyl-*N*-(tertbutyldimethylsilyl)-trifluoroacetamide, and analyzed by capillary gas chromatography–mass spectrometry. Deuterated standards were used to correct for recovery.

Histology Analysis

H&E staining was done at UConn histology core. The histo score was analyzed by pathologist Dr. Michael Goedken, who is a co-author. The total mouse numbers used for histology analysis are: WT CTRL (n=6), WT EtOH (n=6), *Shp*$^{-/-}$ CTRL (n=6), *Shp*$^{-/-}$ EtOH (n=6), *Bhmt*$^{-/-}$ CTRL (n=6), *Bhmt*$^{-/-}$ EtOH (n=8), *Bhmt*$^{-/-}$*Shp*$^{-/-}$ CTRL (n=6), and *Bhmt*$^{-/-}$*Shp*$^{-/-}$ EtOH (n=6).

Statistical analysis

All statistical comparisons were made using Student's t-test, and P values less than 0.05 were considered to be statistically significant. All data are shown as mean ± standard error of mean (SEM) from independent experiments.

Supplementary References

1. Teng YW, Mehedint MG, Garrow TA, et al. Deletion of betaine-homocysteine S-methyltransferase in mice perturbs choline and 1-carbon metabolism, resulting in fatty liver and hepatocellular carcinomas. J Biol Chem 2011;286:36258-67.
2. Wang L, Lee YK, Bundman D, et al. Redundant pathways for negative feedback regulation of bile acid production. Dev Cell 2002;2:721-31.
3. Bertola A, Mathews S, Ki SH, et al. Mouse model of chronic and binge ethanol feeding (the NIAAA model). Nat Protoc 2013;8:627-37.
4. Li Y, Zhang H, Jiang C, et al. Hyperhomocysteinemia promotes insulin resistance by inducing endoplasmic reticulum stress in adipose tissue. J Biol Chem 2013;288:9583-92.
5. Sekiya S, Suzuki A. Direct conversion of mouse fibroblasts to hepatocyte-like cells by defined factors. Nature 2011;475:390-3.
6. Zhang Y, Soto J, Park K, et al. Nuclear receptor SHP, a death receptor that targets mitochondria, induces apoptosis and inhibits tumor growth. Mol Cell Biol 2010;30:1341-56.
7. Smalling RL, Delker DA, Zhang Y, et al. Genome-wide transcriptome analysis identifies novel gene signatures implicated in human chronic liver disease. Am J Physiol Gastrointest Liver Physiol 2013;305:G364-74.
8. Renga B, Mencarelli A, Migliorati M, et al. Bile-acid-activated farnesoid X receptor regulates hydrogen sulfide production and hepatic microcirculation. World J Gastroenterol 2009;15:2097-108.
9. Fiorucci S, Antonelli E, Mencarelli A, et al. The third gas: H2S regulates perfusion pressure in both the isolated and perfused normal rat liver and in cirrhosis. Hepatology 2005;42:539-48.

Supplementary Table 1

qPCR primers		sequences (5' to 3')	chromosomal location (GRCm38)
Bhmt	sense	GCTTAAATGCCGGAGAAGTTG	chr13:93,627,343-93,633,355
	anti-sense	GAACTCCCGATGAAGCTGAC	
Creld2	sense	CTGGTCCAAGCAACAAAGAC	chr15:88,823,094-88,823,816
	anti-sense	TGTACGAGCCGTTGACATTC	
Cth	sense	AGGGTGGCATCTGAATTTGG	chr3:157,913,700-157,918,515
	anti-sense	GTTGGGTTTGTGGGTGTTTC	
Derl1	sense	CGCGATTTAAGGCCTGTTAC	chr15:57,875,529-57,878,495
	anti-sense	TCCCAAGTCCATTGGGTATC	
Ddit3	sense	GCACCTATATCTCATCCCCAG	chr10:127,295,447-127,295,807
	anti-sense	TGCGTGTGACCTCTGTTG	
Herpud1	sense	ATTCTGGGAAGCTGCTGTTG	chr8:94,389,381-94,390,720
	anti-sense	ACCCTTTGTGCTGGTTTCTG	
Hprt1	sense	CGTCGTGATTAGCGATGATGA	chrX:52,988,244-53,002,154
	anti-sense	CACACAGAGGGCCACAATGT	
ChIP primers		**sequences (5' to 3')**	**chromosomal location (GRCm38)**
Bhmt	forward	GTTCCGCAGGAGGAAAATAG	chr13:93,638,286-93,638,435
	reverse	TGGCGATTCATGATAATTCC	
Bhmt 4kbp	forward	AAGGGACAGAAGAACAGAGCAG	chr13:93,641,820-93,641,978
	reverse	GTTGGCATGAAAGCACACAC	
Cth	forward	TGGAAGGTGATTGTGTCTGG	chr3:157,925,743-157,925,897
	reverse	CAGCCCGAACCTAAAACTTTG	
Cth 4kbp	forward	AAGAACCAGGACATGCCATC	chr3:157,928,925-157,929,044
	reverse	TGTGCATGTAGTGTGCCAAG	
cloning primers		**sequences (5' to 3') (undeline: ristriction enzyme site)**	**chromosomal location (GRCm38)**
Bhmt-Pro WT	forward	CGTCACGCGTTCTTCCCATCTGCCTG	chr13:93,637,716-93,639,773
	reverse	GCTCCTCGAGATTGGTCTCCTAGATG	
Cth-Pro -2k	forward	CTCGACGCGTCAAACATAAAAGGCATGCAG	chr3:157,925,046-157,927,074
Cth-Pro -.8k	forward	CTCGACGCGTGAAGGTGATTGTGTCTGGAGC	chr3:157,925,046-157,925,895
Cth-Pro -.7k	forward	CTCGACGCGTAGCTTTTCCAAACCGTAG	chr3:157,925,046-157,925,840
Cth-Pro -.5k	forward	CTCGACGCGTCTGACTCCCTCTTCTGGTGTG	chr3:157,925,046-157,925,641
	reverse	GGAGCTCGAGGTGTTGCTTTGGC	
FoxA1	forward	GTCGAAGCTTATGTTAGGGACTGTGAAGATGG	chr12:57,542,027-57,545,735
	reverse	GTGCGAATTCTAGGAAGTATTTAGCACGGGTC	
FoxA2	forward	GTCGAAGCTTATGCTGGGAGCCGTGAAG	chr2:148,043,514-148,045,895
	reverse	GTGCGAATTCTTAGGATGAGTTCATAATAGGCCTG	
mutagenesis		**sequences (5' to 3') (undeline: mutation site)**	
Bhmt-Pro Mut	forward	CCTCCAGTGCTTATTTGTTGTCTTTAAGCCCTTACTAATATGTTGGGCAGTTTTTGTAG	
	reverse	CTACAAAAACTGCCCAACATATTAGTAAGGGCTTAAAGACAACAAATAAGCACTGGAGG	

Supplementary Fig. 1

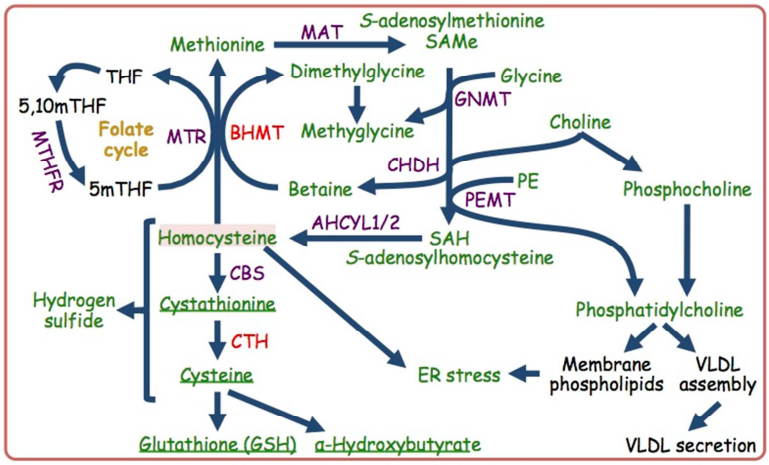

Supp Figure 1.
Homocysteine is known as an endoplasmic reticulum (ER) stress inducer. BHMT (betaine-homocysteine S-methyltransferase) and CTH (cystathionine γ-lyase) are enzymes responsible for the remethylation and transsulfuration pathways, respectively, of homocysteine metabolism in the liver. (AHCYL; adenosylhomocysteinase-like; CBS, cystathionine β-synthase; CHDH, choline dehydrogenase; GNMT, glycine N-methyltransferase; MAT, methionine adenosyltransferase; MTHFR, methylenetetrahydrofolate reductase; MTR, methionine synthase; PEMT, phosphatidylethanolamine N-methyltransferase; 5mTHF, 5-methyltetrahydrofolate; 5,10mTHF 5,10-methylenetetrahydrofolate; THF, tetrahydrofolate)

Supplementary Fig. 2A

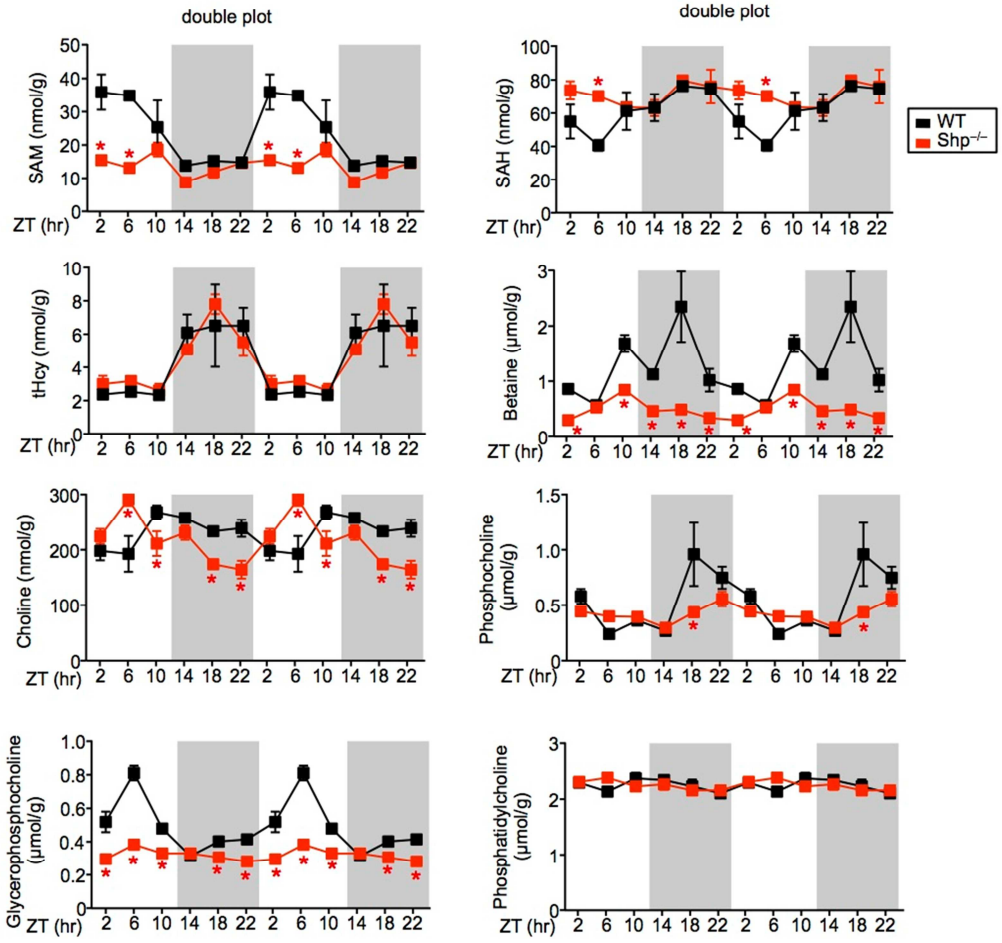

Supp Figure 2A.
Double plot of liver metabolites in WT (black) and *Shp*$^{-/-}$ (red) mice shown in Fig. 1e. Data are shown in mean ± SEM (n=5 mice/group with triplicate assays). *$P < 0.01$, *Shp*$^{-/-}$ vs WT.

Supplementary Fig. 2B

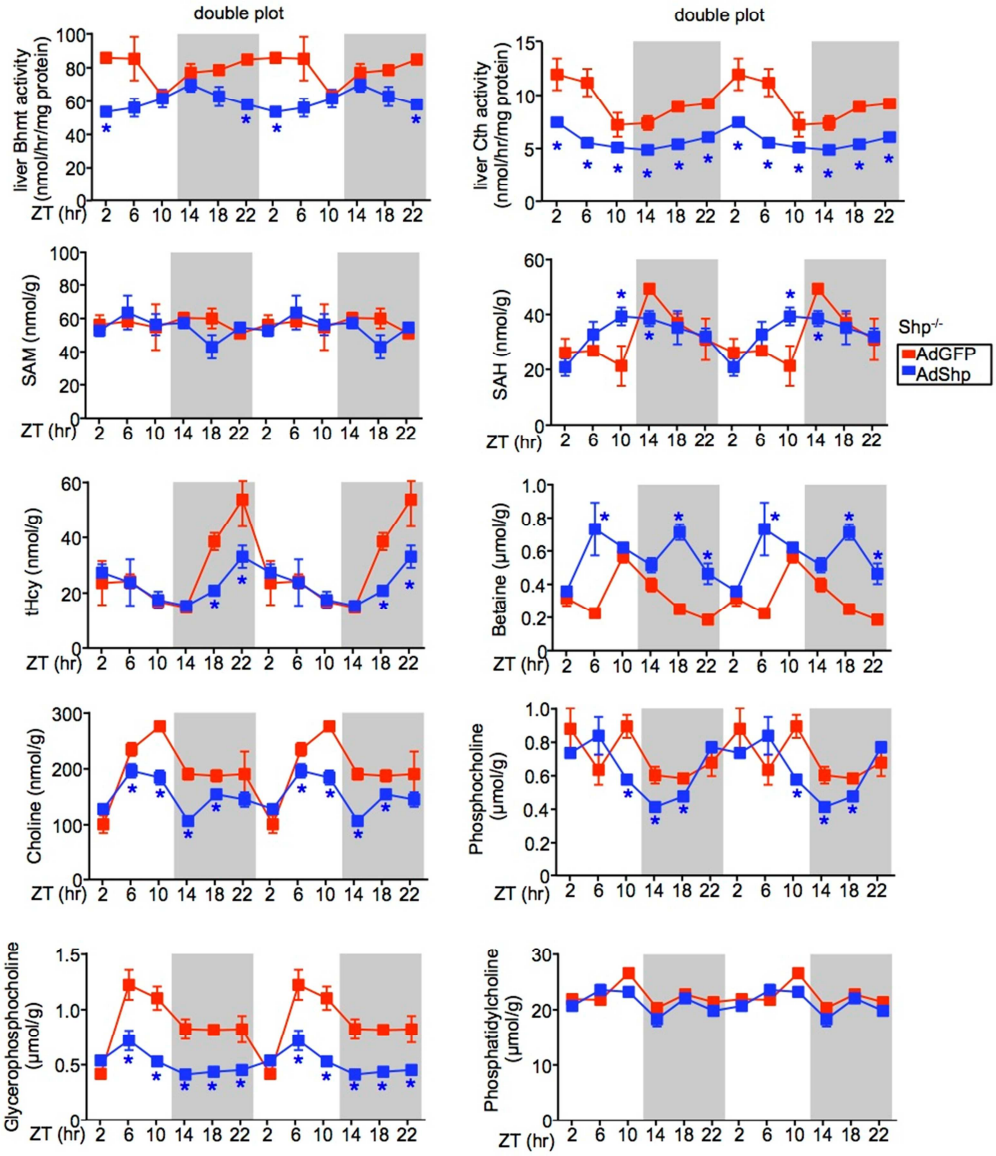

Supp Figure 2B.
Double plot of enzymatic activities of hepatic Bhmt and Cth (*top*) and liver metabolites in *Shp*$^{-/-}$ mice that were re-expressed with GFP (red) or Shp-adenovirus (blue). *$P < 0.01$, AdShp vs AdGFP. Each ZT time point represents pooled samples from 5 individual mice.

Supplementary Fig. 3

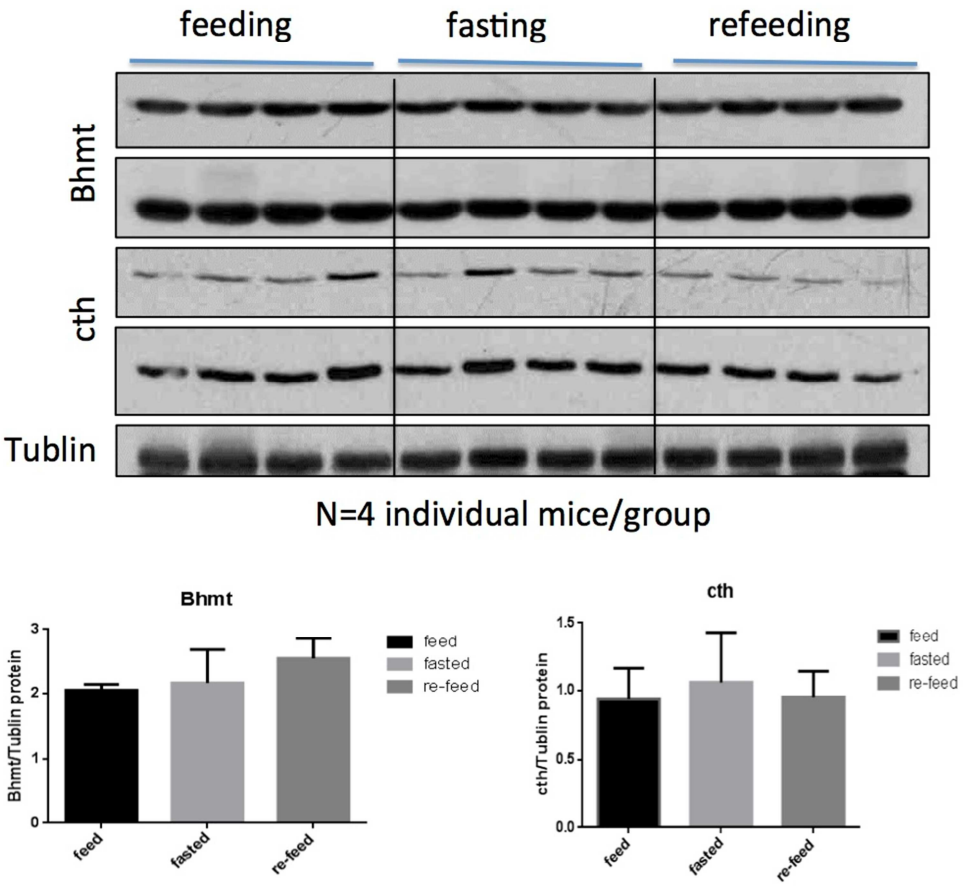

Supp Figure 3.
Western blot of Bhmt and Cth proteins in WT mice under feeding, fasting and refeeding conditions. Samples were collected at ZT12/6 pm (fed), ZT4/10 am (fasted for 16 hr from 6 pm to 10 am) and ZT8/2 pm (4 hr refed from 10 am to 2 pm). Top: each line represents a single mouse and 4 individual mice/group are presented. Two different exposure times for Bhmt and Cth are shown. Bottom: quantification of band intensity for each protein. No significant differences are observed for Bhmt and Cth proteins among the experimental groups.

Supplementary Fig. 4

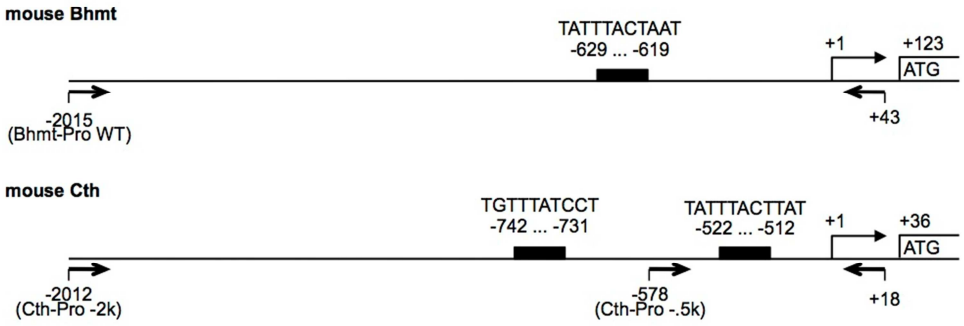

Supp Figure 4a.
Putative FOXA1-binding sites in the mouse Bhmt and Cth promoters. Bold arrows indicate the PCR primers for the construction of reporter vectors used in **Fig. 3**.

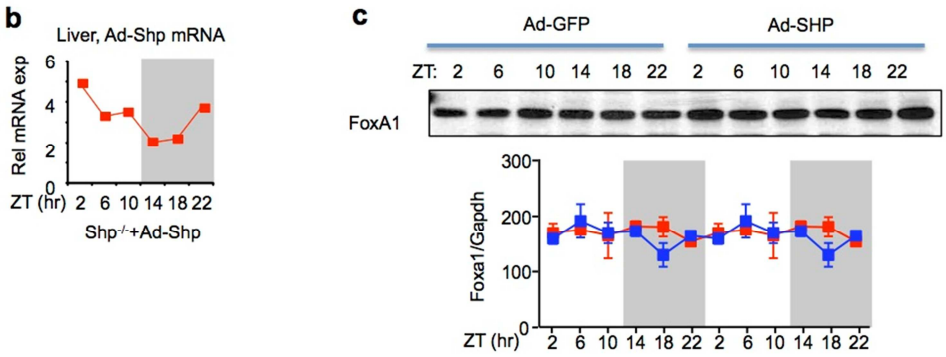

Supp Figure 4b-4c. qPCR of Shp mRNA (a) and WB of FoxA1 protein (b, top) in $Shp^{-/-}$ liver with Shp re-expression using adenovirus (Ad) mediated gene delivery over the 12h/12h light/dark cycle. 4b bottom: Double plot of hepatic Foxa1 mRNA in *Shp*$^{-/-}$ mice that were re-expressed with GFP (red) or Shp-adenovirus (blue). Each ZT time point represents pooled samples from 5 individual mice.

Supplementary Fig. 5

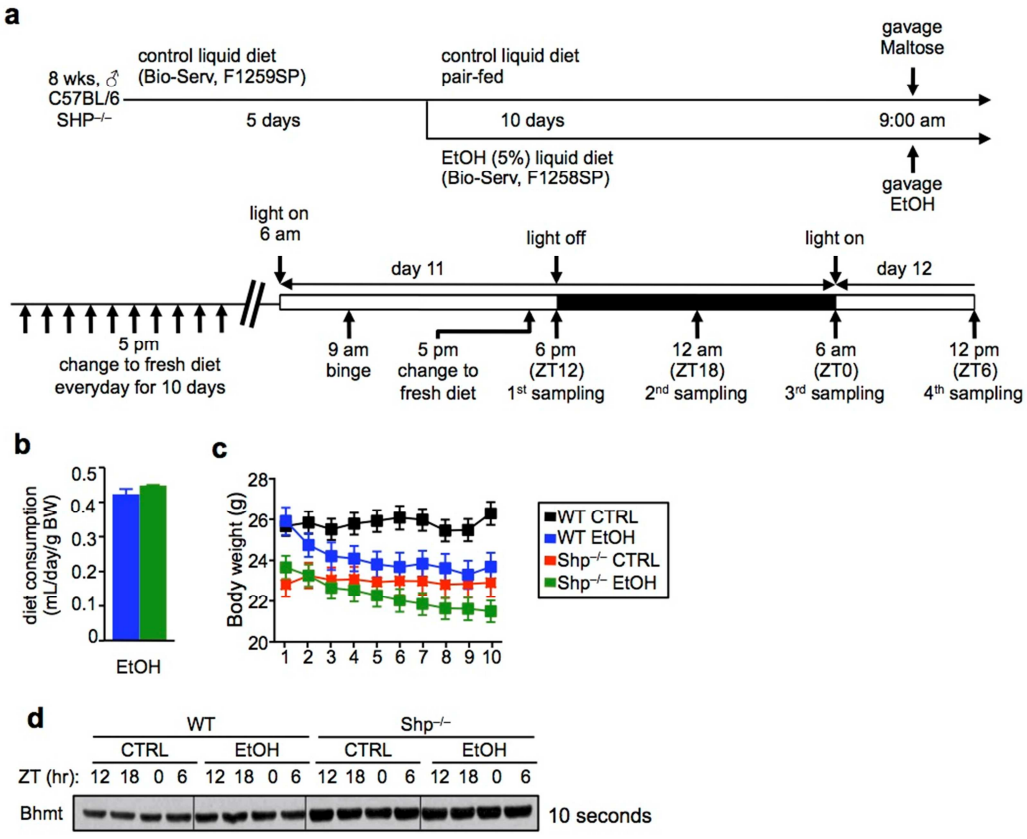

Supp Figure 5.
a. Mouse model of chronic and binge ethanol feeding (*Nat. Protoc.* **8**, 627–637, 2013). After acclimatization for 5 days, the mice were given control (CTRL) or ethanol-containing (EtOH) Lieber-DeCarli liquid diets for 10 days, followed by oral gavage of maltose (CTRL) or ethanol (EtOH) solutions at 9 am on day 10. Nine hours after the binge (ZT 12; 6 pm), liver tissues and blood samples were collected every 6 hour for 24 hours. ZT, Zeitgeber time.
b. Diet consumption of WT EtOH (blue) and Shp$^{-/-}$ EtOH (dark green) mice.
c. Changes in body weight (BW) of WT CTRL (black), WT EtOH (blue), Shp$^{-/-}$ CTRL (red) and Shp$^{-/-}$ EtOH (dark green) mice (n = 12).
d. WB of Bhmt with a longer exposure time. The blot in the main Fig. 4d was exposed for 3 seconds.

Supplementary Fig. 6A

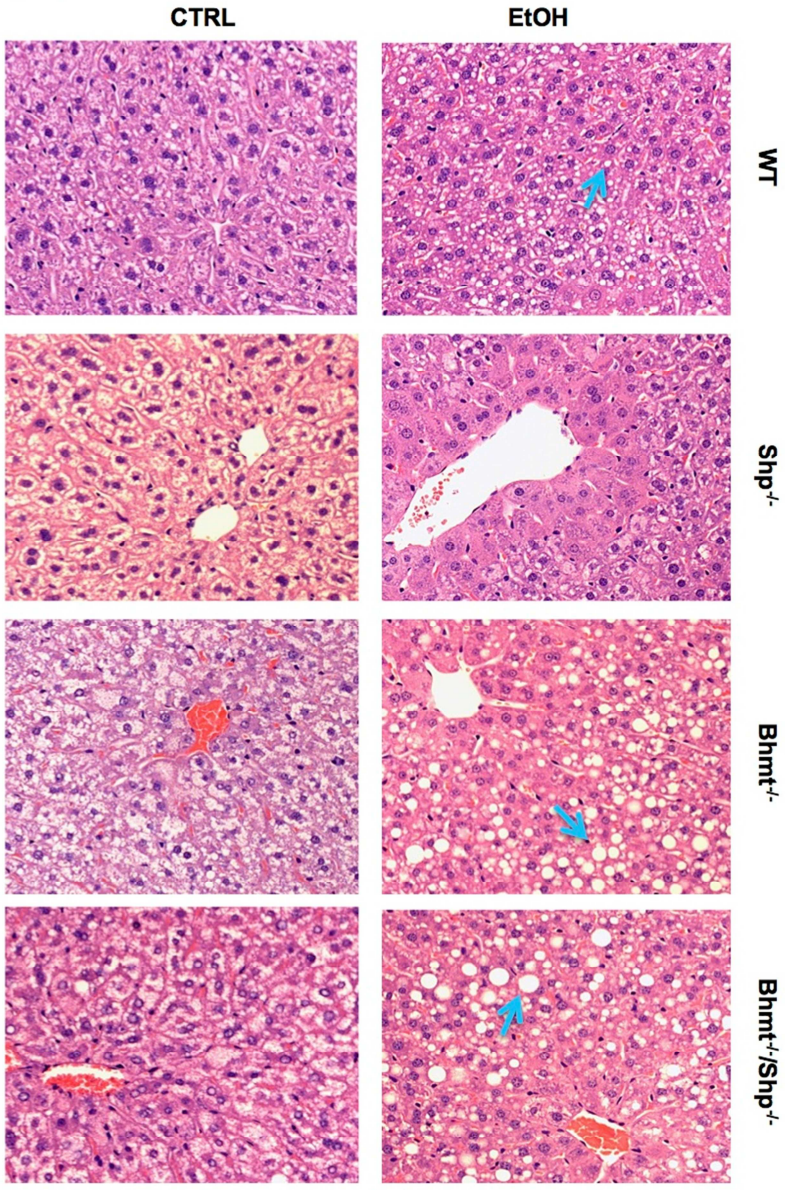

Supp Figure 6A.
H&E staining of liver sections in WT, Shp-/-, Bhmt-/-, and Bhmt-/-/Shp-/- mice fed with control liquid/maltose-binge or ethanol-binge diet. 10X magnification. Macrovesicular fatty change is characterized by a single large fat droplet within each liver cell (blue arrow). Microvesicular fatty change is characterized by multiple small fat droplets that accumulate and expand the hepatocytes.

Supplementary Fig. 6B

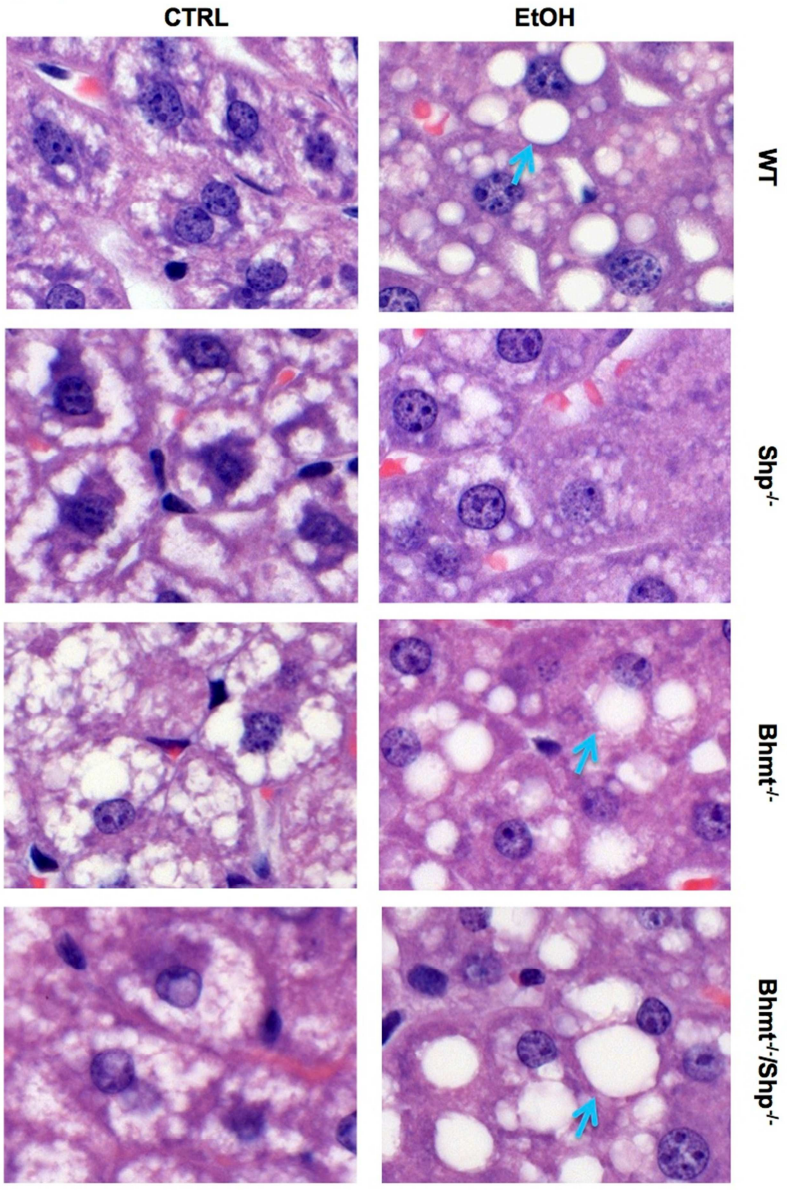

Supp Figure 6B.
H&E staining of liver sections in WT, Shp-/-, Bhmt-/-, and Bhmt-/-/Shp-/- mice fed with control liquid/maltose-binge or ethanol-binge diet. 40X magnification. Macrovesicular fatty change is characterized by a single large fat droplet within each liver cell (blue arrow). Microvesicular fatty change is characterized by multiple small fat droplets that accumulate and expand the hepatocytes.

Supplementary Fig. 6C

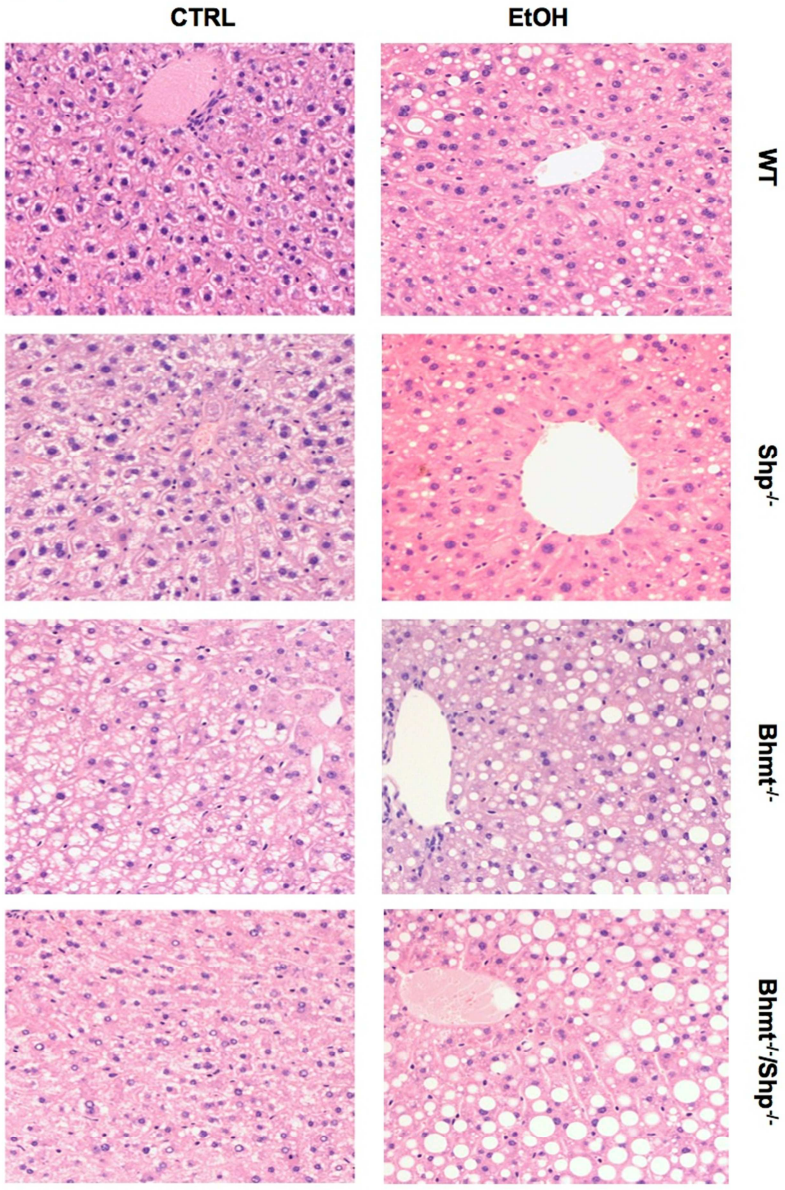

Supp Figure 6C.
H&E staining of liver sections in WT, Shp-/-, Bhmt-/-, and Bhmt-/-/Shp-/- mice fed with control liquid/maltose-binge or ethanol-binge diet. 10X magnification. Macrovesicular fatty change is characterized by a single large fat droplet within each liver cell (blue arrow). Microvesicular fatty change is characterized by multiple small fat droplets that accumulate and expand the hepatocytes.

Supplementary Fig. 6D

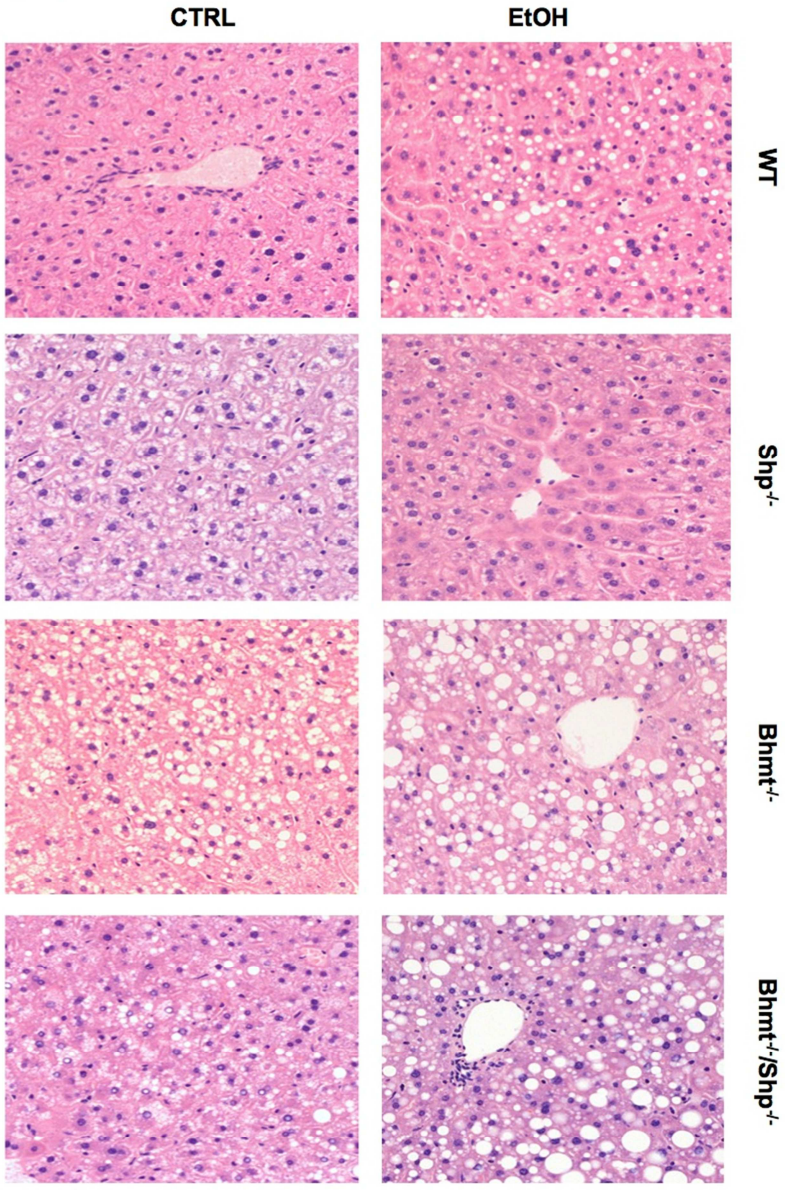

Supp Figure 6D.
H&E staining of liver sections in WT, Shp-/-, Bhmt-/-, and Bhmt-/-/Shp-/- mice fed with control liquid/maltose-binge or ethanol-binge diet. 10X magnification. Macrovesicular fatty change is characterized by a single large fat droplet within each liver cell (blue arrow). Microvesicular fatty change is characterized by multiple small fat droplets that accumulate and expand the hepatocytes.